

Atomic Structure Calculations for Pb^{+70} and Pb^{+71}

G.G. KONAN^{a,*} AND B. KARAÇOBAN USTA^b

^a*Department of Physics, Science Faculty, Sakarya University, 54050, Sakarya, Turkey*

^b*Department of Engineering Fundamental Science, Sakarya University of Applied Sciences, 54050, Sakarya, Turkey*

Received: 15.08.2022 & Accepted: 3.10.2022

Doi: [10.12693/APhysPolA.142.539](https://doi.org/10.12693/APhysPolA.142.539)

*e-mail: ggunday@sakarya.edu.tr

This paper describes a detailed theoretical analysis of energies, Landé g -factors, lifetimes for excited levels, and wavelengths, transition probabilities, and weighted oscillator strengths for electric dipole transitions for Mg- and Na-like lead. Recently, the accurate atomic knowledge of highly ionized heavy atoms has been attractive for many fields, such as laser physics and astrophysics. We used two independent atomic codes to determine atomic data. These are a Hartree–Fock code including superposition of configurations with relativistic corrections, and AUTOSTRUCTURE code which includes Breit interactions and quantum electrodynamics contributions. The calculated data were compared graphically with available works in order to confirm the reliability of our results. In general, we reached a good agreement. The obtained new atomic data for Pb ions were not reported before. This study provides a reference for analyzing astrophysical spectra.

topics: relativistic corrections, wavelengths, oscillator strengths, transition probabilities

1. Introduction

In recent years, there has been considerable interest in the research on highly ionized high- Z elements. Accurate atomic data for these ions are necessary not only for atomic physics but also for many fields of science and technology, such as plasma physics, laser physics, astrophysics, fusion applications, etc. Heavy elements are used in fusion environments, and their spectra supply important information on plasma parameters [1–3]. On the other hand, Na-like ions with a valence electron and Mg-like ions with two valence electrons out of a closed core are convenient systems for theoretical calculations.

In the past few years, some calculations have been employed to determine atomic data about Mg-like ions. These data have been studied following various relativistic approaches. But there is a lack of complete energy levels and transition data for upper levels of Mg-like Pb (Pb^{+70} , $Z = 82$). Recently, Hu et al. [4] calculated the $n = 3$ to $n' = 3$ transitions using multiconfiguration Dirac–Hartree–Fock (MCDHF) and relativistic configuration interaction (RCI) method in the Mg isoelectronic sequence of Pb. Santana and Träbert [5, 6] reported the relativistic multi-reference Møller–Plesset (MR–MP) many-body perturbation theory calculations for $3s3p$, $3p^2$, $3s3d$, $3p3d$, and $3d^2$ levels in Mg-like Pb. Energy levels and electric dipole (E1), electric

quadrupole (E2), magnetic dipole (M1), and magnetic quadrupole (M2) transition parameters were presented by employing the fully relativistic model-potential Flexible Atomic Code (FAC) by Iorga and Stancalie [7].

For Na-like Pb (Pb^{+71} , $Z = 82$) ion, there is no detailed data for energy levels and transition parameters in the literature. Seely and Wagner [8] reported quantum electrodynamics (QED) contributions to the $3s$ – $3p$ transitions in highly charged Na-like ions. Resonance transition energies of Na-like ions were presented by Kim et al. [9]. E1, E2, and M1 transition probabilities among states with principal quantum numbers $n = 3$ and 4 were computed using Dirac–Fock single-configuration wave functions for Na-like Pb ion by Baik et al. [10]. Blundell [11] calculated the screened self-energy and vacuum polarization in Na-like ions. Beiersdorfer and Wargelin [12] made a measurement of the $3s_{1/2}$ – $3p_{3/2}$ transition energies in Na-like Pb. Simionovici et al. [13] reported on $n = 3$ to $n' = 3$ soft-X-ray transitions for Na-like Pb. Johnson et al. [14] presented transition probabilities for Na-like ions. Transition energies of the D lines in Na-like ions were investigated by Gillaspay et al. [15]. Sapirstein and Cheng performed S -matrix calculations of energy levels of Na-like ions [16]. Relativistic distorted-wave collision strengths and oscillator strengths for $\Delta n = 0$ transitions in Na-like ions were computed by Fontes and Zhang [17].

In this study, a consistent data set of energy levels, Landé g -factors, lifetimes, wavelengths, weighted oscillator strengths, and transition probabilities for E1 transitions are reported for Mg-like Pb (Pb⁺⁷⁰, $Z = 82$) and Na-like Pb (Pb⁺⁷¹, $Z = 82$). Na-like ions are essential to the diagnostics of fusion energy devices [18] and in astronomy [19]. Also, Mg-like ions are highly useful in the characterization of astrophysical and laboratory plasmas based on temperature and electron density [20, 21]. The ground state configuration for Pb⁷⁰⁺ and Pb⁷¹⁺ ions are [Ne]3s² and [Ne]3s, respectively. The AUTOSTRUCTURE (AUTOS.) and pseudo-relativistic Hartree–Fock (HFR) atomic codes have been used for the calculations. The HFR method considers the correlation effects and relativistic corrections. The AUTOSTRUCTURE results include contributions of QED (i.e., self-energy and vacuum polarization) and Breit interaction (magnetic interaction between the electrons and retardation effects of the electron–electron interaction), as well as correlation effects (valence–valence (VV), core–valence (CV), and core–core (CC)), which are significant for investigations involving the electronic structure and spectroscopic properties of many-electron systems. In addition, the electron correlation effects due to the Coulomb interaction between the electrons are also important, particularly on fine structure and transitions.

2. Calculation method

The AUTOSTRUCTURE code developed by Badnell [22] and the pseudo-relativistic Hartree–Fock method developed by Cowan (Cowan’s HFR method) [23] have been used in the calculations.

The theoretical basis of these methods was described in detail in [24, 25] and was applied successfully in previous works by our working group [26, 27]. So we only briefly summarize it here.

In HFR and AUTOSTRUCTURE, wave functions are calculated with the Breit–Pauli relativistic corrections. This Hamiltonian can be written as

$$H_{\text{BP}} = H_{\text{NR}} + H_{\text{RC}}, \quad (1)$$

where H_{NR} is the usual nonrelativistic Hamiltonian

$$H_{\text{NR}} = \sum_{i=1}^N h(i) + \sum_{j>i=1}^N \frac{1}{r_{ij}} = \sum_{i=1}^N \left(-\frac{1}{2} \nabla_i^2 - \frac{Z}{r_i} \right) + \sum_{j>i=1}^N \frac{1}{r_{ij}}, \quad (2)$$

and H_{RC} contains the relativistic correction operators, which include one-body relativistic operators (spin–orbit interaction, the non-fine-structure mass variation, and the one-body Darwin corrections) and two-body Breit operators (spin–other–orbit, the mutual spin–spin, the spin–spin contact, the two-body Darwin, and the orbit–orbit terms). Unlike in AUTOSTRUCTURE, two-body operators are neglected in HFR Hamiltonian.

In AUTOSTRUCTURE atomic code, the probability for spontaneous emission by electric dipole (E1) radiation is

$$A_{i' \rightarrow i} = 2.6774 \times 10^9 \frac{(E_i - E_{i'})}{g_i} S(i, i'), \quad (3)$$

where g_i is statistically weighted of level, E_i and $E_{i'}$ are energies of levels, and $S(i, i')$ is line strength in the form

$$S(i, i') = \left| \left\langle i' \left\| R^{[k]} \right\| i \right\rangle \right|^2, \quad (4)$$

where $R^{[k]}$ is a transition operator and describes each multipole, and k is 1 for electric dipole radiation.

The weighted absorption or emission oscillator strength (gf) value can be written in terms of line strength

$$(gf)_{i,i'} = (gf)_{i',i} = \frac{|E_i - E_{i'}|}{3} S(i, i'). \quad (5)$$

According to the HFR method, the total electric dipole (E1) transition probability from a state $\gamma' J' M'$ to all states M levels of γJ is given by

$$A_{E1} = \frac{64\pi^4 e^2 a_0^2 \sigma^3}{3h(2J' + 1)} \mathbf{S} \quad (6)$$

and absorption oscillator strength is given by

$$f_{ij} = \frac{2(E_j - E_i)}{3(2J + 1)} \mathbf{S}, \quad (7)$$

where \mathbf{S} is the electric dipole line strength

$$\mathbf{S} = \left| \left\langle \gamma J \left\| \mathbf{P}^{(1)} \right\| \gamma' J' \right\rangle \right|^2 \quad (8)$$

in atomic units of $e^2 a_0^2$ and $\sigma = [(E_j - E_i)/hc]$ has units of kaysers [cm^{-1}].

Most experiments yield the lifetime of the upper level because of easy measuring. In this case, the sum over multipole transitions to all lower-lying levels must be taken. The lifetime τ for a level j is defined as follows

$$\tau_j = \frac{1}{\sum_i A_{ji}}. \quad (9)$$

3. Results and discussion

Herein, we have calculated the energies, Landé g -factors, lifetimes, and radiative parameters such as wavelengths (λ [\AA]), weighted oscillator strengths (gf), and transition probabilities (A_{ji} [s^{-1}]) for electric dipole (E1) transitions in Mg-like Pb (Pb⁷⁰⁺) and Na-like Pb (Pb⁷¹⁺) using AUTOSTRUCTURE [22] and HFR codes [23]. The results of this work are given in Tables I–III and Figs. 1–10, where they are compared with available data. In the tables, the odd-parity states are indicated by the superscript “*o*”, and we have omitted the filled subshells $1s^2 2s^2 2p^6$ neon core. References to values from other sources are given below the tables with a superscript lowercase letter. Also, the new results of this work are presented in Tables SI and SII in the supplementary material [28].

TABLE I

Energies (E), Landé g -factors, and lifetimes (τ) of $3l3l'$ ($l, l' = 0, 1, 2$) levels for Pb^{+70} . Numbers in brackets represent powers of 10.

No.	Levels		E [cm $^{-1}$]					g -factors	τ [ps]
			This work		Other works			This work	This work
			AUTOS.	HFR	MR-MP ^a	MCDHF ^b	FAC ^c	HFR	HFR
1	$3s^2$	1S_0	0	0	0	0	0	0.00	–
2	$3s3p$	$^3P_0^o$	1343818	1200873	1334575	1331878.95	1375895.00	0.00	4.81(1)
3	$3s3p$	$^3P_1^o$	1500378	1353251	1482132	1479906.43	1529201.67	1.35	–
4	$3p^2$	3P_0	3200074	2901703	3169969	3166216.05	3274475.00	0.00	7.16
5	$3s3p$	$^3P_2^o$	6217690	6404664	6202117	6207723.27	6411120.83	1.50	–
6	$3s3p$	$^1P_1^o$	6560248	6733537	6540902	6547518.69	6763793.33	1.15	1.41(–1)
7	$3p^2$	1D_2	7911664	7929577	7880116	7881581.37	8142199.17	1.14	1.70
8	$3p^2$	3P_1	7938150	7974678	7905770	7909397.39	8171566.67	1.50	1.88(–1)
9	$3s3d$	3D_1	8173869	8099180	8167706	8166791.60	8440541.67	0.50	2.42(–1)
10	$3s3d$	3D_2	8322194	8263856	8304962	8306724.29	8585741.67	1.15	1.19(–1)
11	$3s3d$	3D_3	9301419	9249595	9247132	9247166.97	9553800.00	1.33	2.98
12	$3s3d$	1D_2	9460716	9398671	9400531	9402006.50	9714791.67	1.06	1.41
13	$3p3d$	$^3F_2^o$	9620348	9423204	9601282	9598047.72	9917333.33	0.76	1.92(1)
14	$3p3d$	$^3D_1^o$	9940094	9710509	9924305	9922234.43	10254616.67	0.83	1.80(–1)
15	$3p3d$	$^3P_2^o$	10918203	10722091	10857093	10855019.19	11214358.33	1.29	2.58
16	$3p3d$	$^1F_3^o$	10960933	10758213	10888930	10887409.72	11248058.33	1.11	3.59
17	$3p^2$	3P_2	12873296	13233776	12834575	12846829.49	13270550.00	1.33	9.74(–2)
18	$3p^2$	1S_0	13048548	13401802	13013624	13026622.64	13457616.67	0.00	9.95(–2)
19	$3p3d$	$^3D_2^o$	14611831	14727677	14593954	14599119.26	15083000.00	1.05	1.10(–1)
20	$3p3d$	$^3P_0^o$	14695356	14803921	14685641	14691012.56	15178183.33	0.00	1.07(–1)
21	$3p3d$	$^3P_1^o$	14702882	14821044	14689103	14694527.52	15178758.33	1.10	1.08(–1)
22	$3p3d$	$^3F_3^o$	14712004	14822909	14684532	14690569.04	15182291.67	1.09	1.17(–1)
23	$3p3d$	$^3F_4^o$	15637580	15762455	15568121	15574212.72	16086716.67	1.25	2.13(–1)
24	$3p3d$	$^1D_2^o$	15734312	15868709	15673256	15679392.33	16196116.67	1.23	1.86(–1)
25	$3p3d$	$^3D_3^o$	15907442	16044103	15837129	15844243.02	16367533.33	1.22	1.84(–1)
26	$3p3d$	$^1P_1^o$	16015680	16149968	15954199	15962150.72	16489983.33	1.07	1.71(–1)
27	$3d^2$	3F_2	16463366	16330756	16465337	16464114.86	17017616.67	0.78	1.25(–1)
28	$3d^2$	3P_0	16698417	16556452	16713272	16713454.77	17277975.00	0.00	1.15(–1)
29	$3d^2$	3F_3	17553252	17439206	17505641	17505051.37	18088658.33	1.08	2.35(–1)
30	$3d^2$	3P_2	17652457	17542820	17614691	17614585.22	18203216.67	1.17	2.18(–1)
31	$3d^2$	1G_4	17701661	17576267	17636804	17637361.77	18226100.00	1.06	2.58(–1)
32	$3d^2$	3P_1	17698190	17580539	17667324	17667137.19	18258183.33	1.50	2.13(–1)
33	$3d^2$	3F_4	18726421	18627708	18625763	18626536.64	19243775.00	1.19	1.70
34	$3d^2$	1D_2	18808471	18714370	18723513	18724644.26	19346483.33	1.21	1.38
35	$3d^2$	1S_0	19059722	18951604	18980213	18983704.87	19616808.33	0.00	9.91(–1)

^a Ref. [6], ^b Ref. [4], ^c Ref. [7]

3.1. Mg-like Pb

In our AUTOSTRUCTURE calculation, we have included valance–valance, core–valance, and core–core correlations and the configurations: $3lnl'$ ($l = 0-2$, $n = 3-6$, $l' = 0-4$), $2p^53s^23l$ ($l = 1-2$), $2p^53s3p^2$, $2p^53p^3$, $2p^53s^24s$, $2p^53s3p3d$, $2p^53p^23d$, $2p^53s3p4s$, $2p^53l3d^2$ ($l = 0-2$), $2p^53p3d4s$, $2s2p^53s^23p3d$, $2p^43s3p^3$, $2p^43s^23l3l'$ ($l = 1-2$, $l' = 1-2$).

For HFR calculation, we have taken into account only the configurations including one electron excitation from valence to other subshells: $3s^2$, $3p^2$, $3d^2$, $3snd$ ($n = 3-8$), $3sns$ ($n = 4-8$), $3sng$ ($n = 5-8$), $3sni$ ($n = 7, 8$), $3pnp$ ($n = 4-8$), $3pnf$ ($n = 4-8$), $3pnh$ ($n = 6-8$), $3snp$ ($n = 3-8$), $3snf$ ($n = 4-8$), $3snh$ ($n = 6-8$), $3pnd$ ($n = 3-8$), $3pnd$ ($n = 3-8$), $3pns$ ($n = 4-8$), $3pms$ ($n = 4-8$), $3png$ ($n = 5-8$). In the calculation, the Hamiltonian's calculated eigenvalues were not optimized to the observed energy

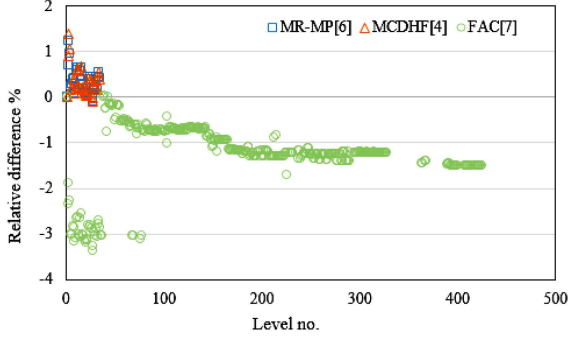


Fig. 1. The percentage differences between the present energies (AUTOSTRUCTURE) and other theoretical results for Mg-like Pb [4, 6, 7].

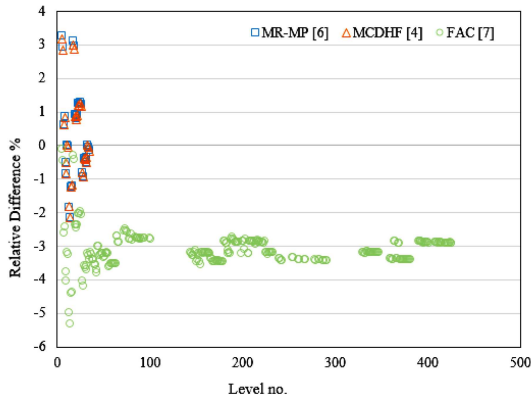


Fig. 2. The percentage differences between the present energies (HFR) and other theoretical results for Mg-like Pb [4, 6, 7].

levels via a least-squares fitting (LSF) procedure using experimentally determined energy levels. That was because experimentally determined energy levels are not available in the literature for Pb^{+70} . The scaling factors of the Slater parameters (F^k and G^k) and configuration interaction integrals (R^k) that were not optimized in LSF , were chosen as 0.95 for calculation, while the spin-orbit parameters were left at their initial values. The calculated HFR results are reported as *ab initio* results (Tables I–III, SI–SII).

In Table I, we have listed only the energy levels, Landé g -factors, and lifetimes (τ) of $3l3l'$ ($l, l' = 0, 1, 2$) levels for Pb^{+70} . The energy levels are relative to the $3s^2 \ ^1S_0$ ground state. As can be seen in Table I, the results obtained from the AUTOS. and HFR calculations are in agreement with the results obtained from MR–MP [6], MCDHF [4], and FAC [7]. We have calculated the differences in percent ($(|E_{\text{present}} - E_{\text{others}}|/E_{\text{others}}) \times 100$) to assess the accuracy of our results for all levels. The percent differences between AUTOS. results from our and other works [4, 6, 7] are in the range of 0.01–3.35%. When the differences between our HFR results and theoretical data of [4, 6, 7] are in

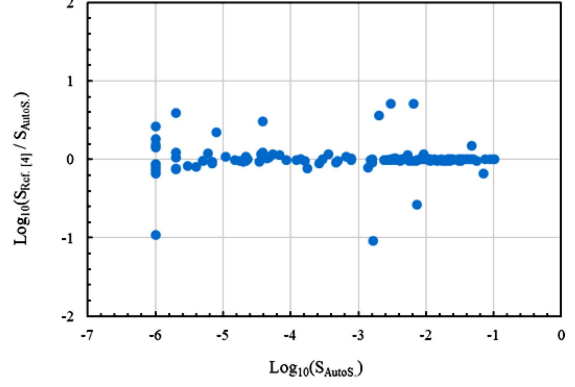


Fig. 3. Comparison of the present $\log(S)$ calculated in this work (AUTOSTRUCTURE) with those of Hu et al. [4] for E1 transitions of Mg-like Pb.

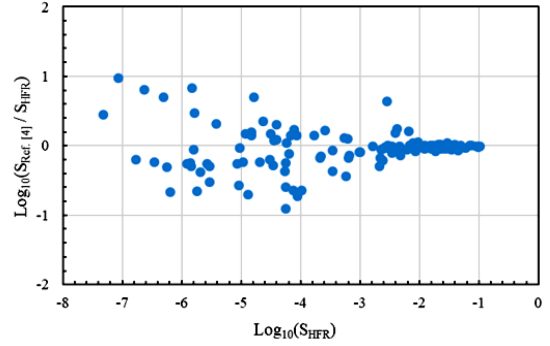


Fig. 4. Comparison of the present $\log(S)$ calculated in this work (HFR) with those of Hu et al. [4] for E1 transitions of Mg-like Pb.

the range of 0.01–5.30% (except for the $3s3p \ ^3P_{0,1}^o$ and $3p^2 \ ^3P_0$ levels, where the differences are up to 8.35–12.73%). We have also graphically compared our results with the results obtained from MR–MP [6], MCDHF [4], and FAC [7] for all levels. The percentage of the relative differences ($(E_{\text{present}} - E_{\text{others}})/E_{\text{others}}\%$) with the MR–MP, MCDHF, and FAC results is illustrated in Figs. 1 and 2. Figure 2 does not include the energies values of $3s3p \ ^3P_{0,1}^o$ and $3p^2 \ ^3P_0$ levels. As seen in these figures, the energy results obtained from our calculations are in agreement with the available results.

Weighted oscillator strengths (gf) and transition probabilities (A_{ij} [s^{-1}]) for E1 transitions between the levels of $3l3l'$ ($l, l' = 0, 1, 2$) in Pb^{+70} are graphically compared (Figs. 3–7). Figures 3 and 4 show $\log_{10}(S_{\text{OW}}/S_{\text{TW}})$ as a function of line strength $\log_{10}(S_{\text{TW}})$ for E1 transitions in, respectively, AUTOSTRUCTURE and HFR calculations. Using the uncertainty estimation method suggested by Kramida [29, 30], we estimated the uncertainties of S -values for E1 transitions using an estimator $dS = \log_{10}(S_{\text{OW}}/S_{\text{TW}})$, where OW means other work and TW means this work. Here, we refer to the

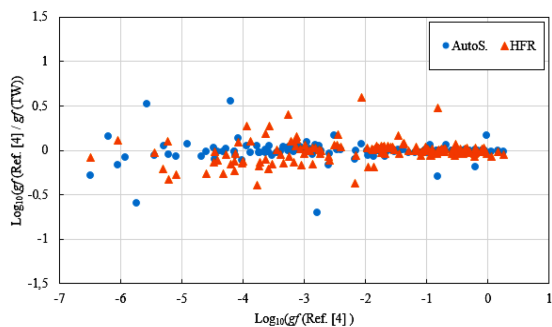


Fig. 5. Comparison of the present $\log(gf)$ calculated in this work (TW: AUTOSTRUCTURE and HFR) with those of Hu et al. [4] for E1 transitions of Mg-like Pb.

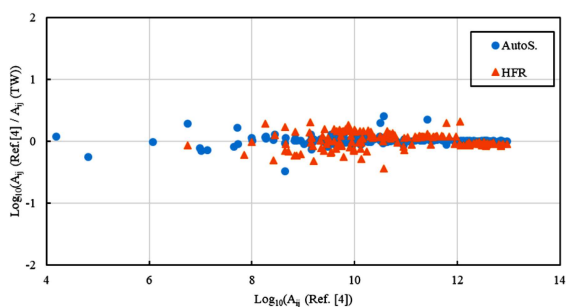


Fig. 6. Comparison of the present $\log_{10}(A_{ij})$ calculated in this work (TW: AUTOSTRUCTURE and HFR) with those of Hu et al. [4] for E1 transitions of Mg-like Pb.

results given in [4] and compared to our AUTOS. and HFR results. The root mean square (rms) of dS is equal to $\sqrt{dS^2}$, and percentage uncertainty is estimated as $u\% = (10^{\text{rms}} - 1) \times 100$. According to Figs. 3 and 4, if few outliers are excluded, the agreement between $\log_{10}(S_{\text{OW}})$ and $\log_{10}(S_{\text{TW}})$ for the E1 transitions with ($\log_{10} S_{\text{TW}} \geq -2.17$) is 8.5% for AUTOS. and 7.7% for HFR.

The gf computed in the present work ($\log(gf)$ (AUTOS.) and $\log(gf)$ (HFR)) for the E1 transitions between the levels of $3l3l'$ ($l, l' = 0, 1, 2$) in Pb^{+70} are compared with the available results from [4] in Fig. 5. The comparison shows that our results agree with those of [4]. If these few outliers are excluded, the rms value of $\log_{10}(gf)$ ($[4]/(gf)$ (AUTOS.)) for these transitions is 0.111. This corresponds to an average difference of about 29%. For HFR calculation, the rms value (0.097) of the relative differences reaches 25%, from [4], except for some transitions. Also, the comparison of the transitions between our transition probabilities (A_{ij}) and MCDHF [4] (calculation B) and FAC results [7] has been displayed in Figs. 6 and 7. As seen in Figs. 6 and 7, our transition probabilities agree with [4] and [7], except for some transitions. The rms value of the relative differences between our results and other works has been found in the val-

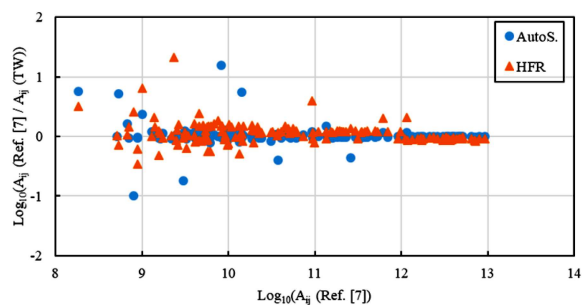


Fig. 7. Comparison of the present $\log_{10}(A_{ij})$ calculated in this work (TW: AUTOSTRUCTURE and HFR) with those of Iorga et al. [7] for E1 transitions of Mg-like Pb.

ues 19% and 26% for the comparison of AUTOS. with [4, 7] and 33% and 31% for the comparison of HFR with [4, 7], respectively, except for some transitions. The agreement between the presented data is strong evidence for the reliability of the HFR and AUTOS. calculations for gf and A_{ij} .

3.2. Na-like Pb

We have considered the nl ($n = 3-6$, $l = 0-5$), $2p^5 3snl$ ($n = 3-5$, $l = 0-4$), $2p^5 3pnl$ ($n = 3-5$, $l = 0-4$), $2p^5 3dnl$ ($n = 3-5$, $l = 0-4$), $2p^4 3s^2 3p$, $2p^4 3s^2 3d$, $2s 2p^5 3s^2 3p$ configurations in AUTOSTRUCTURE calculation and the nl ($n = 3-15$, $l = 0-6$) configurations in the HFR calculation. These configurations have been considered for correlation effects (including VV, CV, and CC correlations in AUTOSTRUCTURE and VV correlation in HFR). According to the configurations mentioned, we have obtained 1630 energy levels for AUTOSTRUCTURE and 149 energy levels for HFR.

In HFR calculation, the Hamiltonian's calculated eigenvalues were optimized to the observed energy levels via a least-squares fitting (LSF) procedure using experimentally determined energy levels, specifically the two levels from [12]. The scaling factors of the Slater parameters (F^k and G^k) and configuration interaction integrals (R^k), not optimized in the least-squares fitting, were chosen as 0.95 for calculation, while the spin-orbit parameters were left at their initial values.

Table II gives the energies, Landé g -factors, and lifetimes of nl ($n \leq 6$, $l \leq 5$) levels for Pb^{+71} . The energy levels are relative to the $3s^2 S_{1/2}$ ground state. References for other comparison values are typed with a superscript lowercase letter. There are only $3l$ and $4l$ levels for this ion in the literature for comparison. As can be seen in Table II, our results are in agreement with other works. We have calculated the mean ratio (AUTOSTRUCTURE/HFR) for the accuracy of our results. The mean ratio of energy levels for our HFR and AUTOS. calculations is 1.02. The agreement between the presented data is strong evidence for the reliability of the HFR

TABLE II

Energies (E), Landé g -factors, and lifetimes (τ) of nl ($n \leq 6$, $l \leq 5$) levels for Pb^{+71} . Numbers in brackets represent powers of 10.

No.	Levels		E [cm^{-1}]			g -factors	τ [ps]
			This work		Other works	This work	This work
	Conf.	Term	AUTOS.	HFR		HFR	HFR
1	3s	$^2S_{1/2}$	0	0	0	2.00	
2	3p	$^2P_{1/2}^o$	1531666	1518510	1526564.76 ^a 1519049 ^b 1518695 ^c 1518499.22 ^d 1518511.8 ^e 1518015.28 ^g 1506569 ^h 1549447.37 ⁱ	0.67	1.67(1)
3	3p	$^2P_{3/2}^o$	6449362	6442050	6448399.23 ^a 644008 ^b 6445375 ^c 6442430.73 ^d 6442541.5 ^e 6442053.7 ^f 6442430.73 ^g 6429044 ^h 6443127.58 ⁱ	1.33	2.19(-1)
4	3d	$^2D_{3/2}$	8145982	8087830	8167972.36 ^a 8142811 ^h	0.80	2.77(-1)
5	3d	$^2D_{5/2}$	9292945	9253130	9263272.69 ^a 9241948 ^h	1.20	2.96
6	4s	$^2S_{1/2}$	34299810	33761050	33743224 ^h	2.00	8.24(-3)
7	4p	$^2P_{1/2}^o$	34868176	34313330	34361919 ^h	0.67	1.18(-2)
8	4p	$^2P_{3/2}^o$	36940192	36481360	36378593 ^h	1.33	9.81(-3)
9	4d	$^2D_{3/2}$	37588305	37025510	37028326 ^h	0.80	4.22(-3)
10	4d	$^2D_{5/2}$	38088391	37522830	37503102 ^h	1.20	5.93(-3)
11	4f	$^2F_{5/2}^o$	38423299	37852510	37836122 ^h	0.86	2.41(-3)
12	4f	$^2F_{7/2}^o$	38636524	38066530	38045817 ^h	1.14	2.64(-3)
13	5s	$^2S_{1/2}$	49299019	48747650	–	2.00	1.08(-2)
14	5p	$^2P_{1/2}^o$	49628877	49021180	–	0.67	1.38(-2)
15	5p	$^2P_{3/2}^o$	50642356	50113930	–	1.33	1.25(-2)
16	5d	$^2D_{3/2}$	50943313	50379920	–	0.80	6.14(-3)
17	5d	$^2D_{5/2}$	51200551	50635190	–	1.20	8.04(-3)
18	5f	$^2F_{5/2}^o$	51364737	50798940	–	0.86	4.70(-3)
19	5f	$^2F_{7/2}^o$	51474829	50909260	–	1.14	5.06(-3)
20	5g	$^2G_{7/2}$	51496672	50930510	–	0.89	8.43(-3)
21	5g	$^2G_{9/2}$	51561172	50994810	–	1.11	8.71(-3)
22	6s	$^2S_{1/2}$	58341822	56673250	–	2.00	1.57(-2)
23	6p	$^2P_{1/2}^o$	58551381	56826800	–	0.67	1.90(-2)
24	6p	$^2P_{3/2}^o$	59117679	57452130	–	1.33	1.78(-2)
25	6d	$^2D_{3/2}$	59279145	57602150	–	0.80	9.44(-3)
26	6d	$^2D_{5/2}$	59427640	57749880	–	1.20	1.19(-2)

TABLE II cont.

No.	Levels		E [cm $^{-1}$]			g -factors	τ [ps]
			This work		Other works	This work	This work
	Conf.	Term	AUTOS.	HFR		HFR	HFR
27	6 <i>f</i>	$^2F_{7/2}^o$	59519547	57842910	–	0.86	8.09(–3)
28	6 <i>f</i>	$^2F_{7/2}^o$	59583983	57906960	–	1.14	8.61(–3)
29	6 <i>g</i>	$^2G_{7/2}$	59597377	57921010	–	0.89	1.46(–2)
30	6 <i>g</i>	$^2G_{9/2}$	59634820	57958360	–	1.11	1.50(–2)
31	6 <i>h</i>	$^2H_{9/2}^o$	59635186	57959520	–	0.91	2.22(–2)
32	6 <i>h</i>	$^2H_{11/2}^o$	59659933	57984160	–	1.09	2.26(–2)

^aRef. [17], ^bRef. [9], ^cRef. [8], ^dRef. [11], ^eRef. [15], ^fRef. [12], ^gRef. [16], ^hRef. [10], ⁱRef. [14]

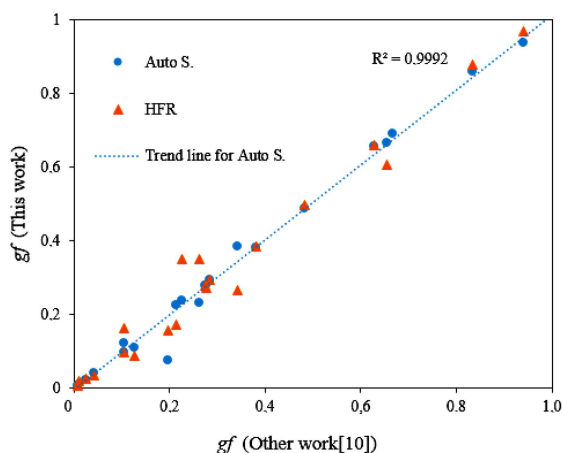


Fig. 8. Comparison of the weighted oscillator strengths calculated in this work (AUTOSTRUCTURE and HFR) with those of Baik et al. [10] for E1 transitions of Na-like Pb.

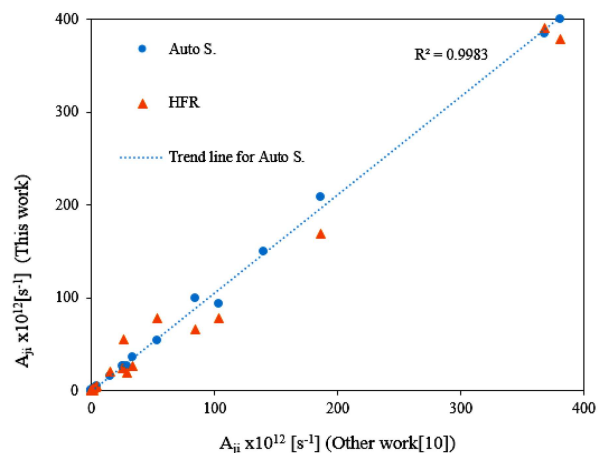


Fig. 9. Comparison of the transition probabilities calculated in this work (AUTOSTRUCTURE and HFR) with those of Baik et al. [10] for E1 transitions of Na-like Pb.

and AUTOS. calculations. Also, the energies, Landé g -factors, and lifetimes of upper levels, which are new results, are given in the supplementary material in Table SI [28] for HFR calculation.

We have obtained 339316 and 2296 possible E1 transitions for the selected configurations in the AUTOS. and HFR calculations, respectively. Transition probabilities (A_{ji} [s $^{-1}$]), weighted oscillator strengths (gf), wavelengths (λ [Å]), and line strengths (S [a. u.]) for E1 transitions between the levels of $3l$ ($l = 0, 1, 2$) and $4l$ ($l = 0, 1, 2, 3$) are listed in Table III. In this table, the number in brackets represents the power of 10. Our results are in good agreement with other works [8–10, 14, 17], as seen in Table III. We have calculated the mean ratio gf (this work)/ gf (other work) for the accuracy of our results. The mean ratio between our results and other works [10] has been found in the values 0.99 and 1.07 for AUTOS. and HFR calculations, respectively. As seen in Table III, the results obtained from the AUTOS. and HFR calculations are in agreement with other works within transition probabilities results. We have found the

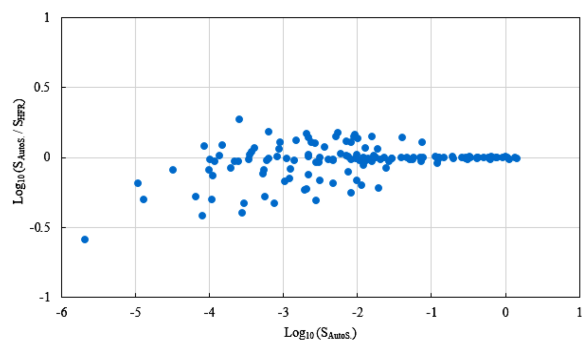


Fig. 10. Comparison of line strengths derived in this work from the AUTOSTRUCTURE calculations with the HFR calculations for E1 transitions of Na-like Pb.

values 1.02 and 1.07 for the mean ratio of A_{ji} (this work)/ A_{ji} [10], respectively. Also, gf and A_{ji} comparisons of the E1 transitions have been presented in, respectively, Figs. 8 and 9 (except the transition 2.82 Å (in HFR)).

TABLE III

Transition probabilities (A_{ji}), weighted oscillator strengths (gf), and wavelengths (λ) for electric dipole (E1) transitions between the levels of $3l$ ($l = 0, 1, 2$) and $4l$ ($l = 0, 1, 2, 3$) in Pb^{+71} . Numbers in brackets represent powers of 10.

Transitions				Method	A_{ji} [s^{-1}]		gf		λ [\AA]		S [a. u.]
Upper level	Lower level				This work	Other works	This work	Other works	This work	Other works	This work
3p	$^2P_{1/2}^o$	3s	$^2S_{1/2}$	AUTOS.	5.75(10)	3.515(10) ^a	7.35(-2)	7.02(-2) ^b	65.29	65.854 ^d	1.58(-2)
				HFR	5.98(10)	5.375(10) ^b	7.77(-2)	7.1142(-2) ^c	65.85	65.846 ^e	1.69(-2)
3p	$^2P_{3/2}^o$	3s	$^2S_{1/2}$	AUTOS.	4.56(12)	4.569(12) ^a	6.57(-1)	6.628(-1) ^a	15.51	15.5218 ^d	1.68(-2)
				HFR	4.56(12)	4.545(12) ^b	6.59(-1)	6.6484(-1) ^c	15.52	15.515 ^e	1.68(-2)
3d	$^2D_{3/2}$	3p	$^2P_{1/2}^o$	AUTOS.	3.55(12)	3.542(12) ^a	4.87(-1)	4.822(-1) ^a	15.12	-	1.21(-2)
				HFR	3.95(12)		4.99(-1)	4.8272(-1) ^c	15.22		1.37(-2)
3d	$^2D_{3/2}$	3p	$^2P_{3/2}^o$	AUTOS.	1.17(10)	1.204(10) ^a	2.43(-2)	2.458(-2) ^a	58.94	-	4.73(-3)
				HFR	1.13(10)		2.50(-2)	2.4672(-2) ^c	60.76		5.00(-3)
3d	$^2D_{5/2}$	3p	$^2P_{3/2}^o$	AUTOS.	3.43(11)	3.355(11) ^a	3.82(-1)	3.814(-1) ^a	35.17	-	2.95(-2)
				HFR	3.38(11)		3.84(-1)	3.8162(-1) ^c	35.57		3.00(-2)
4s	$^2S_{1/2}$	3p	$^2P_{1/2}^o$	AUTOS.	2.71(13)	2.663(13) ^a	7.55(-2)	1.968(-1) ^a	3.05	-	0.76(-3)
				HFR	5.48(13)	2.767(13) ^b	1.58(-1)		3.10		1.61(-3)
4s	$^2S_{1/2}$	3p	$^2P_{3/2}^o$	AUTOS.	9.95(13)	8.486(13) ^a	3.85(-1)	3.410(-1) ^a	3.59	-	9.09(-3)
				HFR	6.66(13)	8.594(13) ^b	2.68(-1)		3.66		6.45(-3)
4p	$^2P_{1/2}^o$	3s	$^2S_{1/2}$	AUTOS.	9.42(13)	1.034(14) ^a	2.32(-1)	2.626(-1) ^a	2.87	-	2.20(-3)
				HFR	7.80(13)		3.51(-1)		2.74		1.58(-3)
4p	$^2P_{1/2}^o$	3d	$^2D_{3/2}$	AUTOS.	2.65(13)	2.922(13) ^a	1.11(-1)	1.274(-1) ^a	3.74	-	2.74(-3)
				HFR	2.00(13)		8.73(-2)		3.81		2.18(-3)
4p	$^2P_{1/2}^o$	4s	$^2S_{1/2}$	AUTOS.	1.05(10)	1.325(12) ^a	9.76(-2)	1.038(-1) ^a	175.94	-	5.64(-2)
				HFR	1.00(10)		9.83(-2)		181.07		5.86(-2)
4p	$^2P_{3/2}^o$	3s	$^2S_{1/2}$	AUTOS.	5.43(13)	5.388(13) ^a	2.39(-1)	2.258(-1) ^a	2.71	-	1.07(-3)
				HFR	7.80(13)		3.51(-1)		2.74		1.58(-3)
4p	$^2P_{3/2}^o$	3d	$^2D_{3/2}$	AUTOS.	1.33(12)	1.428(12) ^a	9.63(-3)	1.074(-2) ^a	3.47	-	1.10(-4)
				HFR	2.54(12)		1.89(-2)		3.52		2.19(-4)
4p	$^2P_{3/2}^o$	3d	$^2D_{5/2}$	AUTOS.	1.59(13)	1.551(13) ^a	1.24(-1)	1.052(-1) ^a	3.62	-	2.23(-3)
				HFR	2.02(13)		1.63(-1)		3.67		2.96(-3)
4p	$^2P_{3/2}^o$	4s	$^2S_{1/2}$	AUTOS.	1.09(12)	1.090(12) ^a	9.37(-1)	9.416(-1) ^a	37.87	-	5.84(-2)
				HFR	1.20(12)		9.69(-1)		36.76		5.88(-2)
4d	$^2D_{3/2}$	3p	$^2P_{1/2}^o$	AUTOS.	1.50(14)	1.400(14) ^a	6.90(-1)	6.656(-1) ^a	2.77	-	3.15(-3)
				HFR	2.09(14)		9.96(-1)		2.82		4.63(-3)
4d	$^2D_{3/2}$	3p	$^2P_{3/2}^o$	AUTOS.	3.65(13)	3,320(13) ^a	2.26(-1)	2.126(-1) ^a	3.21	-	2.38(-3)
				HFR	2.68(13)		1.72(-1)		3.27		1.85(-3)
4d	$^2D_{3/2}$	4p	$^2P_{1/2}^o$	AUTOS.	1.06(12)	9.878(11) ^a	8.59(-1)	8.332(-1) ^a	36.76	-	5.20(-2)
				HFR	1.08(12)		8.78(-1)		36.87		5.34(-2)
4d	$^2D_{3/2}$	4p	$^2P_{3/2}^o$	AUTOS.	2.85(9)	2.863(9) ^a	4.07(-2)	4.064(-2) ^a	154.29	-	2.07(-2)
				HFR	1.74(9)		3.53(-2)		183.77		2.13(-2)
4d	$^2D_{5/2}$	3p	$^2P_{3/2}^o$	AUTOS.	2.09(14)	1.862(14) ^a	1.87(0)	1.734(0) ^a	3.16	-	1.30(-2)
				HFR	1.69(14)		1.57(0)		3.22		1.11(-2)
4d	$^2D_{5/2}$	4p	$^2P_{3/2}^o$	AUTOS.	9.76(10)	9.208(10) ^a	6.66(-1)	6.550(-1) ^a	87.09	-	1.27(-1)
				HFR	7.32(10)		6.07(-1)		96.02		1.28(-1)
4f	$^2F_{5/2}^o$	3d	$^2D_{3/2}$	AUTOS.	3.85(14)	3.682(14) ^a	3.78(0)	3.756(0) ^a	3.30	-	2.73(-2)
				HFR	3.90(14)		3.96(0)		3.36		2.92(-2)
4f	$^2F_{5/2}^o$	3d	$^2D_{5/2}$	AUTOS.	2.63(13)	2.511(13) ^a	2.79(-1)	2.762(-1) ^a	3.43	-	3.14(-3)
				HFR	2.47(13)		2.72(-1)		3.50		3.14(-3)
4f	$^2F_{5/2}^o$	4d	$^2D_{3/2}$	AUTOS.	2.30(10)	2.066(10) ^a	2.96(-1)	2.848(-1) ^a	119.76	-	7.80(-2)
				HFR	2.25(10)		2.96(-1)		120.92		7.85(-2)

TABLE III cont.

Transitions				Method	A_{ji} [s^{-1}]		gf		λ [\AA]		S [a. u.]
Upper level	Lower level				This work	Other works	This work	Other works	This work	Other works	This work
4f	$^2F_{5/2}^o$	4d	$^2D_{5/2}$	AUTOS.	1.04(8)	1.015(8) ^a	8.32(-3)	8.232(-3) ^a	298.59	–	8.20(-3)
				HFR	1.02(8)		8.42(-3)		303.32		8.43(-3)
4f	$^2F_{7/2}^o$	3d	$^2D_{5/2}$	AUTOS.	4.00(14)	3.807(14) ^a	5.58(0)	5.503(0) ^a	3.41	–	4.70(-2)
				HFR	3.79(14)		5.48(0)		3.47		4.69(-2)
4f	$^2F_{7/2}^o$	4d	$^2D_{5/2}$	AUTOS.	6.95(9)	6.740(9) ^a	2.78(-1)	2.744(-1) ^a	182.44	–	1.25(-1)
				HFR	6.84(9)		2.78(-1)		183.93		1.26(-1)

^aRef. [10], ^bRef. [14], ^cRef. [18], ^dRef. [17], ^eRef. [9]

Transition data for E1 transitions from principal quantum numbers $n = 5$ and $n = 6$ to lower levels are given in the supplementary material in Table SII [28]. These values for these transitions have been presented for the first time. The mean ratio of transition probabilities and weighted oscillator strengths for all our HFR and AUTOS. calculations (Table III and Table SII) are 1.01 and 1.00, respectively, except for the transition $6s\ ^2S_{1/2} - 3p\ ^2P_{1/2}^o$. Also, the line strengths derived from these AUTOS. calculations ($\log_{10}(S_{AUTOS.})$) were compared with the HFR calculation ($\log_{10}(S_{HFR.})$) for our results in Table III and Table SII. The rms value of $\log_{10}(S_{AUTOS.}/S_{HFR.})$ for 78 transitions out of a total of 138 depicted in Fig. 10 is 0.015. This corresponds to a reasonable difference of about 3.5%.

4. Conclusion

In summary, we have performed HFR and AUTOSTRUCTURE calculations for Pb^{+70} and Pb^{+71} . In the presented work, new energies, the Landé g -factors, lifetimes for excited levels, and electric dipole parameters such as transition probabilities, wavelengths, and weighted oscillator strengths are reported in the tables. Also, comparisons with available works have been made graphically as well. The compared results have a good agreement, in general. We believe that our present work may help fill the gap and provide high-accuracy data for highly-ionized heavy ions that are significant for fusion plasma research and astrophysics.

Acknowledgments

The authors are very grateful to the anonymous reviewers for stimulating comments and valuable suggestions, which have resulted in improving the presentation of the paper. Also, we are grateful to Dr. Alexander Kramida for the extensive help with the uncertainty estimation of data in this manuscript.

References

- [1] J. D. Gillaspy, *J. Phys. B: At. Mol. Opt.* **34**, R93 (2001).
- [2] Z.L. Zhao, K. Wang, S. Li, R. Si, C.Y. Chenc, Z.B. Chend, J. Yanb, Y. Ralchenko, *At. Data Nucl. Data Tables* **119**, 314 (2018).
- [3] D. Osin, J.D. Gillaspy, J. Reader, Y. Ralchenko, *Eur. Phys. J. D* **66**, 286 (2012).
- [4] F. Hu, M. Mei, C. Han, B. Han, G. Jiang, J. Yang, *J. Quant. Spectrosc. Radiat. Transfer* **149**, 158 (2014).
- [5] J.A. Santana, E. Träbert, *Phys. Rev. A* **91**, 022503 (2015).
- [6] J.A. Santana, *At. Data Nucl. Data Tables* **111–112**, 87 (2016).
- [7] C. Iorga, V. Stancalie, *At. Data Nucl. Data Tables* **123–124**, 313 (2018).
- [8] J.F. Seely, R.A. Wagner, *Phys. Rev. A* **41**, 5246 (1990).
- [9] Y.K. Kim, D.H. Haik, P. Indelicato, J.P. Desclaux, *Phys. Rev. A* **44**, 148 (1991).
- [10] D.H. Baik, Y.G. Ohr, K.S. Kim, J.M. Lee, P. Indelicato, Y.K. Kim, *At. Data Nucl. Data Tables* **47**, 177 (1991).
- [11] S.A. Blundell, *Phys. Rev. A* **47**, 1790 (1993).
- [12] P. Beiersdorfer, B.J. Wargelin, *Rev. Sci. Instrum.* **65**, 13 (1994).
- [13] A. Simionovici, D.D. Dietrich, R. Keville, T. Cowan, P. Beiersdorfer, M.H. Chen, S.A. Blundell, *Phys. Rev. A* **48**, 3056 (1993).
- [14] W.R. Johnson, Z.W. Liu, J. Sapirstein, *At. Data Nucl. Data Tables* **64**, 279 (1996).
- [15] J.D. Gillaspy, D. Osin, Y. Ralchenko, J. Reader, S.A. Blundell, *Phys. Rev. A* **87**, 062503 (2013).
- [16] J. Sapirstein, K.T. Cheng, *Phys. Rev. A* **91**, 062508 (2015).

- [17] C.J. Fontes, H.L. Zhang, *At. Data Nucl. Data Tables* **113**, 293 (2017).
- [18] U. Feldman, J.F. Seely, E. Landi, Y. Ralchenko, *Nucl. Fusion* **48**, 045004 (2008).
- [19] J.M. Laming U. Feldman, *Astrophys. J.* **527**, 461 (1999).
- [20] E. Hinnov, *Phys. Rev. A* **14**, 1533 (1976).
- [21] I. Martinson, A. Gaupp, *Phys. Rep.* **15**, 113 (1974).
- [22] N.R. Badnell, *Comput. Phys. Commun.* **182**, 1528 (2011).
- [23] Cormac McGuinness, R.D. Cowan's *Atomic Structure Code*, 2009.
- [24] N.R. Badnell, *J. Phys. B* **19**, 3827 (1986).
- [25] R.D. Cowan, *The Theory of Atomic Structure and Spectra*, Univ. of California Press, Berkeley (CA) 1981.
- [26] G.G. Konan, L. Özdemir, *Acta Phys. Pol. A* **137**, 289 (2020).
- [27] B. Karaçoban Usta, S. Eser, *Acta Phys. Pol. A* **137**, 1187 (2021).
- [28] G.G. Konan, B. Karaçoban Usta, *Acta Phys. Pol. A* **142**, 539.S1 (2022).
- [29] A. Kramida, *Fusion Sci. Technol.* **63**, 313 (2013).
- [30] A. Kramida, Y. Ralchenko, J. Reader, and NIST ASD Team (2021), *NIST Atomic Spectra Database*, ver. 5.9, National Institute of Standards and Technology, Gaithersburg (MD) 2021.